NATIONAL AERONAUTICS AND SPACE ADMINISTRATION

Lewis Research Center, Cleveland, Ohio

25p

LEWIS TECHNICAL PREPRINT 9-63 ~~X64 10933~~ N65-89018 Code 2A

(NASA TMX-51292)

# ALUMINA SIZE DISTRIBUTIONS FROM HIGH-PRESSURE COMPOSITE SOLID-PROPELLANT COMBUSTION

By Louis A. Povinelli and Robert A. Rosenstein

[1964] 25p refs Presented at the AIAA

Prepared for

The Solid Propellant Rocket Conference ~~Sponsored by the American Institute of Aeronautics and Astronautics~~

Palo Alto, ~~California~~ 29-31 ~~January 29-31~~, 1964

E-2355

# ALUMINA SIZE DISTRIBUTIONS FROM HIGH-PRESSURE COMPOSITE SOLID-PROPELLANT COMBUSTION

By Louis A. Povinelli and Robert A. Rosenstein

Aerospace Technologists
National Aeronautics and Space Administration
Lewis Research Center

## Summary 10933

Alumina size distributions were obtained for both a coarse and a fine oxidizer composite propellant burning in a nitrogen atmosphere over the pressure range from atmospheric to 500 psi. The amount of additive agglomeration was found to be significantly higher for the coarse oxidizer propellant and decreased with increasing pressure to the 0.3 power over the range from atmospheric pressure to 250 psi.

High-speed photographs of the burning propellant surface revealed that the additives moved on the surface with the average particle velocity decreasing with pressure to approximately the 0.3 power over the pressure range from atmospheric to 50 psi. The empirical relation between particle velocity and pressure was used to modify an agglomeration criterion presented previously. Evaluation of the critical aluminum diameter required for agglomeration indicated that both propellant types used in this study should experience some agglomeration over the pressure range studied. The aluminum size required for agglomeration was found to increase with increasing pressure. The experimental findings of the critical aluminum diameter required for agglomeration were in reasonable agreement with the calculated data.

The volume mean diameter of the alumina was found to decrease with increasing pressure, and the data were compared with that in the literature.

AUTHOR

## Introduction

The use of fine metallic powders, such as aluminum, continues to be one of the most effective and utilized techniques for the suppression of combustion instability in solid-propellant rocket engines[1] regardless of the fact that the additive suppression mechanism is still not well in hand. Recent experiments indicated that the increased damping in a solid-propellant system due to the addition of fine metallic powders could be explained by means of a particle damping theory.[2] The fact that this result contradicts earlier references in the field[1,3,4] serves to illustrate the complexity of the problem and reinforces the opinion that the coupling mechanism between the gas-phase oscillations and the combustion process and the suppression of the oscillations with fine metallic particles will not be completely resolved until a more fundamental and detailed understanding of the metallic-solid combustion processes is obtained.

In order to extend our knowledge of the metallic-solid combustion, it is informative to investigate metal additive behavior during actual propellant burning. Although the combustion of the additive by itself provides us with a great deal of information concerning metal behavior[5,6] it is necessary to study the metallic-solid processes in situ. Phenomena such as additive motion and agglomeration on the burning propellant surface not only increased our knowledge of additive behavior but also provide information applicable to damping calculations. It is only by a gradual increase in our library of facts that the additive suppression mechanism will be understood. An understanding of additive motion and agglomeration will also be useful in determining the velocity and thermal lag of the additives in passing through the nozzle, thereby influencing engine performance.[7,8]

This study is concerned with additive behavior close to the burning propellant surface and an attempt at an understanding of additive agglomeration is presented herein. Small strands of polybutadiene-acrylic-acid - ammonium-perchlorate - aluminum (PBAA-AP-Al) propellants were used that have two compositions, predominantly coarse oxidizer and predominantly fine oxidizer size. The alumina was trapped close to the burning surface and size distributions obtained over the pressure range from atmospheric to 500 psi. Several tests were performed with an erosive type of flow across the test strand. The experimental results were used to modify an agglomeration criterion, and the size distributions were compared with other published data.

## Apparatus and Procedure

Propellants. - PBAA-AP-Al propellants of two types were used in this study. The compositions used are given in table 1. The oxidizer used was a blend of fine (11-micron mean-weight diameter) and coarse (85-micron mean-weight diameter) crystals. The particle size distributions of the aluminum additive and oxidizers were obtained with a micromerograph and are given in fig. 1.

Combustion Product Sample Collection. - The propellant sample sizes were 1/2 by 1/2 in. and were 3/8-in. high. No inhibitor was used on the propellant, and the experiments were performed at 70° ±5° F. The solid combustion products were collected on Pyrex slides located 1/4 to 1/2 in. above the burning surface. The apparatus employed was similar to that used previously[9] and is shown schematically in fig. 2(a). The stationary slides were exposed when the slot passed between the propellant and the Pyrex slide. The concentration of products collected for a given propellant depended on the slot size and plate speed and was determined by collecting a suitable number of samples at varying plate speed and slot size and by inspecting the results under a microscope. Visual judgment was used to arrive at a representative sample after sizing several distributions. The exposure time was decreased with increasing pressure, and at atmospheric pressure it was approximately 1/20 sec. Combustion samples were collected for both propel-

lant compositions from atmospheric pressure to 500 psi. The burning occurred in nitrogen with the exception of several tests that were performed in the open atmosphere.

The collection system was enclosed in a pressure vessel (6 in. in diameter by 7 in. high), and the sliding metal plate was pneumatically driven (piston arrangement) through a solenoid-operated valve. The valve was manually operated subsequent to the initiation of burning. Ignition was accomplished with a 10-v hot-wire system. An accumulator tank was connected to the combustion chamber in order to maintain constant pressure burning. Following combustion, the pressure was released slowly (1000 to 0 psi in approx. 2 min) in order not to disturb the collected combustion products. This vent time was subsequently lengthened to approximately 20 min (500 to 0 psi).

Erosive flow. - For the case of end burning with cross flow, 3/4- by 3/4-in. Transite blocks, 1 in. long were drilled (1/2-in.-diam. hole) and filled with the same propellant (but with no Al) as that under test. The experimental arrangement is shown in fig. 2(b). The propellant in the Transite was ignited, and the resulting gas jet, in turn, ignited the test strand. A 1-in. separation was used between the two propellants. The sample was taken after the burning had propagated across the strand surface. These tests were conducted in the open atmosphere.

High-speed photography. - The combustion chamber contained suitable observation sections for photographing the burning propellant surface. An object to image ratio of unity was used for the photographs (4000 fps), which were taken at an angle of approximately 30° to the surface and over the pressure range from atmospheric to 200 psi. The photographs were taken with Double-X film and Tri-X film with a Wratten 47 filter, and infrared film with a Wratten 25 filter. A nitrogen purge was used around the strand.

Size distribution. - The combustion product samples were projected at a magnification of 500 on the viewing plate of a metallurgical microscope and sized with the aid of a X6 eyepiece. The resolution of this system was approximately 1 micron ($\mu$). A minimum of 1000 particles was counted for each propellant type. With the end-burning strands, the sample was analyzed at the center of the Pyrex slide, whereas in the case of end burning with crossflow, the size distribution was made along the slide in the direction of the flow.

Particle motion. - Aluminum particle displacement on the burning propellant surface was estimated by projecting the film at a magnification of 50 on a ruled screen and by observing the displacement for a large number of particles. A particle velocity was then determined at a given pressure, using the average particle displacement and the film speed.

## Results and Discussion

Pressure effect on agglomeration. - The combustion product size distributions obtained for the two types of propellants (predominantly coarse oxidizer and predominantly fine oxidizer propellant) at atmospheric pressure are given in fig. 3, as well as the initial number distribution of the aluminum, which was determined from the weight distribution of fig. 1. The coarse oxidizer propellant yielded particles that were significantly larger than the initial aluminum additive, whereas the fine oxidizer mixture yielded particles that were only slightly larger than the initial size. This effect has been reported previously[9,10] for propellant samples burned in the open atmosphere. The present results are in substantial agreement with reference 9, although a greater percentage of the combustion products are smaller in diameter with the nitrogen environment. The percentage of the total number of particles that agglomerated was approximately equal although the size distribution obtained in the open atmosphere tests showed a more definite break in the distribution than is indicated in fig. 3. This break (change of slope) occurred near the crossover point between the initial aluminum distribution and the combustion product distribution. The amount of agglomeration was taken as the value corresponding to the point where the combustion product distribution crosses the initial aluminum distribution. The computed increase in aluminum diameter, if it is assumed that the aluminum burns completely to $Al_2O_3$ without forming a hollow sphere, is approximately 20 percent, whereas agglomerated particles are as high as 2500 percent of the original mean size.

The percent of agglomerated additives was found to be dependent on the chamber venting time after burning, as indicated in fig. 4 for a combustion pressure of 500 psi. Sufficiently long vent times were required in order to ensure that the collected sample was not disturbed. Evidently, the effect of fast venting time was to remove the smaller products from the combustion sample. The percent agglomeration showed that a maximum of 16 min was required with the test apparatus to reach an equilibrium size distribution (fig. 5). Subsequent combustion samples were collected for venting times of approximately 20 min.

The resulting size distributions of the alumina at 50, 100, 250, and 500 psi are given in figs. 6, 7, 8, and 9, respectively. The amount of agglomeration decreased with increasing pressure as shown in the log-log plot in fig. 10. A straight line with a negative slope of 0.3 appeared to fit the data reasonably well.

Photographic results. - High-speed photographs of the coarse oxidizer propellant obtained in this study revealed that the average additive particle velocity decreased with increasing pressure between atmospheric pressure and 50 psi, as shown in fig. 11. Above this pressure, soot formation obscured the burning propellant surface. An attempt to use high oxidizer propellants was unsuccessful, and it was not possible to obtain useful photographic data with selective filters and film emulsions above 50 psia.

Photographs of the fine oxidizer propellant, which were obtained only at atmospheric pressure, revealed some particle motion although agglomeration was not evident. The mechanism by which the particles are perturbed is not understood.

Agglomeration criteria. - A model for the agglomeration mechanism was presented in reference 9. The criteria for the occurrence of agglomeration utilized three characteristic times in-

volved in the metallic-solid burning process. Agglomeration was assumed to be a surface phenomenon caused by the collision of molten, unoxidized particles of metal.

It was postulated that (1) the particles require a finite period of time to burn $\tau_B$, (2) the particles have a given residence time on the surface $\tau_R$, and (3) a finite time is required for the particles to agglomerate $\tau_A$. (All symbols are defined in the Appendix.) If the time to burn the particle is less than the agglomeration time, the molten metal burns to its oxide. Since the melting temperature of the metallic oxides generally exceeds propellant surface temperature, agglomeration will not occur. If, however, the burning time exceeds the agglomeration time, the molten additive has an opportunity to agglomerate before it burns and to form an oxide shell. This model led to a twofold condition that had to be fulfilled for agglomeration to occur, namely, (1) the metal residence time must exceed the agglomeration time, and (2) the agglomeration time must be less than the burning time. Employing several assumptions regarding the nature of the burning of additive particles (wherein the burning of the aluminum is limited by the diffusion of oxidizing vapors through the binder gases to the additive site), particle motion and particle residence time, resulted in the following expression for the criteria for agglomeration:

$$\frac{\tau_R}{\tau_A} = \frac{\pi}{4} Kn_a d_a^3 > 1 \qquad (1)$$

$$\frac{\tau_B}{\tau_A} = \frac{\pi K n_a d_a^3 \rho_a \xi r}{24 D_{of} C_o} > 1 \qquad (2)$$

where K was assumed given by the expression

$$v = Kr$$

that is, the perturbation velocity of the additive particles, normal to the main gas flow, was assumed to be proportional to the propellant burning rate.

Modification of agglomeration criteria. - The particle velocity data of fig. 11 leads to the following relation between additive perturbation velocity and pressure:

$$v = \frac{K}{p^{n_1}} \qquad (3)$$

In addition, the mean-oxidizer-particle - additive-particle spacing based on the model of reference 9 is $\xi/2$ rather than $\xi$. Substitution of expression (3) and $\xi/2$ into the two ratios discussed in Agglomeration Criteria yields the following modification of expressions (1) and (2):

$$\frac{\pi}{4} \frac{K}{r} \frac{n_a d_a^3}{p^{n_1}} > 1 \qquad (4)$$

$$\frac{\pi K n_a d_a^3 \rho_a \xi}{48 D_{of} C_o p^{n_1}} > 1 \qquad (5)$$

Expressions (4) and (5) may be used to determine the value of the aluminum particles that are necessary in order for agglomeration to occur. A critical diameter of 20 microns was determined previously[9] for the propellants used herein by use of expression (1). Expression (4) indicates that the critical aluminum size for agglomeration increases with the combustion pressure. Substitution of a log relation for the burning rate, namely,

$$r = C_p^{n_2} \qquad (6)$$

yields

$$\frac{\pi K n_a d_a^3}{4 C_p^{n_1+n_2}} > 1 \qquad (7)$$

For the predominantly coarse oxidizer propellant used in this study, $n_1 = 0.32$ and $n_2 = 0.34$; hence,

$$\frac{B n_a d_a^3}{p^{0.64}} > 1 \qquad (8)$$

where $B = \pi K/4C$. Substitution of the numerical value of B, where $K = 0.34$ from fig. 11 and $C = 0.032$ (when r is in in./sec and is p in psia) and $n_a$ (9 percent concentration by weight) yielded a critical aluminum value of 3.5 $\mu$ at atmospheric pressure.

Numerical evaluation of expression (5) was made from the interparticle spacing , the diffusion coefficient based on the relation $T^{3/2}/p$ (0.35 $cm^2$/sec), and $C_o$ was taken as oxygen density at 1200° K. Propellant surface temperature was assumed to be independent of pressure.

The variations of additive diameter with pressure as calculated from expressions (4) and (5) set equal to unity, are shown in fig. 12. The experimental data, taken from the crossover points of the distributions in figs. 3, 6, 7, 8 and 9, are shown for comparison with the calculated values. Since the complete combustion of the aluminum to its oxide occurs with a 20-percent increase in diameter, the experimental data were correspondingly reduced 20 percent. It is noted that the values determined by expression (5) are the critical aluminum diameters necessary for the occurrence of agglomeration in this particular propellant above a pressure of approximately 150 psia. Expression (4) yields a lower critical diameter below this pressure. The slope of the calculated data appears to correspond reasonably well with that of the experimental data, although the level of the experimental data is higher than the calculated level. A reasonable explanation for this difference in level lies in the fact that an overall "diameter" or size of the agglomerate was measured rather than the size of the individual particles in the agglomerated mass. The experimental data plotted in fig. 12, therefore, represent the size of a "particle" whose components include particles having diameters equal to or greater than the critical value. In addition, if the burning of the additive occurs in such a manner as to form hollow spheres, the particle diameters may be increased appreciably, and the experimentally measured diameter may greatly exceed the original size. This behavior of the additive could account for the size difference between the calculated and experimental values of the critical aluminum size.

The small difference in slope between the experimental and calculated curves can be explained

by the fact that the total number of additive particles whose diameter is equal to or greater than the critical value decreases with increasing critical size (viz. increasing pressure). This, naturally, is due to the fact that the additive has a size distribution (fig. 1). Hence, at high pressures the concentration of additive particles equal to or greater than the critical size required for agglomeration is less than the number available at a lower pressure. One would expect, therefore, the smaller slope shown by the experimental data.

In view of limited photographic data on the fine oxidizer propellant, it was assumed that additive motion behavior with pressure was given by expression (3) with the same pressure exponent n and intercept K. The propellant surface temperature was assumed equal to that of the coarse oxidizer propellant as well as the pressure exponent on the burning rate. The calculated variations of critical aluminum diameter with pressure are shown in fig. 13. The calculated values are slightly higher than those obtained for the coarse oxidizer propellant. Expression (5) yields the critical value above 200 psia, whereas expression (4) yields lower values below that pressure. The experimental data do not appear to depend on combustion pressure for this propellant. The most likely explanation appears to be that the additive motion on the fine oxidizer surface is not given correctly by expression (3). Further data are required to establish this relation.

Literature data. - The data of reference 11 show the percentage of additive particles in a thin zone above the propellant surface with diameters in the same range as the original additive sizes. The percentage of particles with diameters greater than the original particle size is highest at the low pressures and high aluminum concentrations in the propellants. The authors of reference 11 concluded that this was an indication of the amount of agglomeration occurring near the propellant surface. These observations are consistent with the results of the present study. The tendency for additives to agglomerate decreases with increasing pressure, with decreasing aluminum concentration, and with decreasing aluminum size. The data of reference 11 as well as the data presented in this report suggest that the amount of agglomeration may not be proportional to $p^{-n}$ at higher pressures (250 psi).

Volume mean diameter as function of pressure. - During the rapid acceleration that takes place in the throat of a rocket engine utilizing propellants with metal additives, velocity and thermal lags develop between the additives and the gas stream. In determining the thrust loss, it is necessary to know the size distribution of the additive, which, in turn, requires sizing a large number of particles over the entire size range present. In view of the wide size range that may occur from solid propellant burning, this task becomes somewhat difficult. In determining the weight distribution, which represents a more important parameter than the number mean for thrust losses, it is important to include all the large particles, since they add up to a considerable amount of the weight present in the system. Figs. 14 and 15 show both the number and volume size distributions of the combustion products at 250 and 500 psi. In both cases, 90 percent of the weight is found to be contained in 2 percent of the total number of particles. The large agglomerates, therefore, are extremely important in determining a mean weight diameter. Fig. 16 shows that the mean volume diameter decreases significantly with increasing combustion pressure.

The opposite pressure behavior has been noted previously,[12] which led to the conclusion that higher rocket efficiency was obtainable with low pressure operation. In order to understand this discrepancy, it is necessary to consider the experiments of reference 12 and the present work in some detail.

The propellants used in reference 12 and the present study were not identical (variations existed in aluminum concentration, particle sizes, and binder type). In addition, the data of reference 12 was obtained from small rocket firings (both with and without a nozzle) inside a large tank, and subsequently collecting the combustion deposits from the tank walls and sizing the combustion products with an electron microscope. Although some previous evidence exists that the size distributions from strand burning are not comparable to those from rocket engine combustion,[13] the data were not conclusive. Therefore, both the data of reference 12 and that of the present study were compared by plotting the normalized number of particles of a given size against the diameter (fig. 17). The data of reference 12 appear to approach a peak but do not extend over a wide size range. The data of the present study, on the other hand, reveal that the particle count did not reach a peak but did include the larger end of the distribution. The comparison also revealed that both the size distributions were obtained from comparable samples having a number median of 0.5 microns and a mass median of approximately 80 microns.

The data of reference 12 were obtained using an electron microscope and sizing all particles larger than 0.1 microns. This would tend to favor the smaller end of the distribution curve as well as including all of the combustion products formed. The particles were counted as individual particles regardless of whether they overlapped or not. Photographs from reference 12 show some particle groupings which, if treated as an agglomerate of particles, are significantly larger in size than the maximum reported. Reference 12 shows that 90 percent of the mass is contained in 20 percent of the particles at 500 psi and in 30 percent of the particles at 277 psi. These values could be significantly influenced by the presence of any additional larger particles. Chemical analysis of the combustion products in reference 12 revealed the presence of $Al_2O_3$ with small amounts of aluminum and iron.

The conclusion reached from the foregoing discussion is that the data of the study of reference 12 would tend to be correct on a number basis rather than a weight basis. In the present study, the data were more nearly on a mass basis. This may be seen from the following discussion.

Prior to obtaining the size distribution of the burned additive in the present study, non-aluminized combustion product samples were obtained at various pressures and subsequently treated for 1 hr in an oxygen stream at 875° K to remove any carbon present. Sample inspection up to a magnification of 850 revealed a large number of submicron particles whose shape was less regular than the burned additive particles. On the basis of

spectrographic analysis and the collection techniques involved, it was concluded that these particles were contaminants (Ca, Cu, Fe, Mg, Na, P, Si, Ti) and that the mixing process and subsequent handling of the propellants were the chief sources of contamination. In obtaining the product size distribution of the aluminized samples, visual discrimination was used in determining whether the particle was aluminum in nature or not. In practice, therefore, all particles slightly less than 1 μ and above were counted. All particles 1.5 μ in diameter or less were grouped together in presenting the size distributions. Electron diffraction patterns obtained from the combustion products of the aluminized propellants revealed only the presence of aluminum oxide. Thus, the size distribution would tend to be correct on a weight basis rather than on a number basis.

The mean number diameter for the data of reference 12 is 0.8 μ and for the present study is 1.6 μ, both showing no dependence on pressure.

End burning with crossflow. - The results of burning the aluminized test strands with a crossflow of hot combustion gases revealed on an almost twofold increase in the amount of additive agglomeration with the coarse oxidizer propellant (fig. 18). In addition, the fine oxidizer propellant showed a significant amount of agglomeration (2 percent). Referring to expression (4), it is seen that increasing $K/rp^n$ or $v/r$; that is, the ratio of the particle perturbation velocity to the propellant burning rate decreases the additive size required for agglomeration. At the low crossflow velocity used in these tests (~25 ft/sec), the propellant burning rate would not be significantly changed. If the flow over the propellant surface did penetrate sufficiently close to the surface to affect particle motion, it could influence the amount of agglomeration. A high-speed film of the burning did not appear to show any sizeable increases in particle motion. The particles most likely to be affected, however, may not have been resolved. The percent agglomeration for the coarse oxidizer propellant is plotted in fig. 10 for comparison with the case of end burning only.

## Summary of Results

Alumina size distributions were obtained for both a coarse and a fine oxidizer composite propellant burning in a nitrogen atmosphere over the pressure range from atmospheric to 500 psi. The amount of additive agglomeration was found to be significantly higher for the coarse oxidizer propellant. The amount of agglomeration decreased with increasing pressure to the 0.3 power over the range from atmospheric pressure to 250 psi.

High-speed photographs of the burning propellant surface revealed that the additives moved on the surface, with the average particle velocity decreasing with pressure to approximately the 0.3 power over the pressure range from atmospheric to 50 psi. The empirical relationship between particle velocity and pressure was used to modify an agglomeration criterion presented previously. Evaluation of the critical aluminum diameter required for agglomeration indicated that both propellant types used in this study should experience some agglomeration over the pressure range studied. The aluminum size required for agglomeration was found to increase with increasing pressure, varying from 3.5 μ at atmospheric pressure to 6.5 μ at 400 psi for the coarse oxidizer propellant. The experiment findings of the critical aluminum diameter required for agglomeration were in reasonable agreement with the calculated data.

The volume mean diameter of the alumina was found to decrease with increasing pressure, and the data were compared with that in the literature.

Propellant strands burned under conditions of erosive flow revealed an almost twofold increase in agglomeration over the nonerosive tests.

## Appendix - Symbols

| | |
|---|---|
| $B$ | constant, $\pi K/4C$ |
| $C$ | burning rate constant |
| $C_o$ | concentration of oxidizer vapors |
| $D_{o,f}$ | diffusion coefficient of oxidizer vapors through fuel vapors |
| $d_a$ | diameter of additive particle |
| $K$ | constant |
| $n$ | pressure exponent |
| $n_a$ | number of additive particles per unit volume |
| $p$ | combustion pressure |
| $r$ | linear regression rate of solid |
| $v$ | perturbation velocity of additive particles |
| $\xi$ | interparticle oxidizer spacing |
| $\rho_a$ | density of additive particle |
| $\tau_A$ | characteristic agglomeration time, $\frac{4}{\pi n_a d_a^2 v}$ |
| $\tau_B$ | characteristic burning (reaction) time, $\frac{\rho_a \xi d_a}{12 D_{o,f} C_o}$ |
| $\tau_R$ | characteristic residence time, $d_a/r$ |

## References


1. McClure, F. T., et al., A General Review of Our State of Knowledge, First Report of the Working Group on Solid Propellant Combustion Instability, TG 371-1, Appl. Phys. Lab, John Hopkins Univ., July 1960.

2. Horton, M. D. and McGie, M. R., Particulate Damping of Oscillatory Combustion, AIAA Journal, vol. 1, no. 6, June 1963, p. 1319.

3. McClure, F. T., et al., Panel Discussion on Solid Propellant Instability, Eighth Symposium (International) on Combustion, Williams & Wilkins Co., 1962, p. 908.

4. Price, E. W., Combustion Instability in Solid Propellant Rocket Motors, Astronaut. Acta, V, 1959, pp. 63-72.

5. Brzustowski, T. A., and Glassman, I., Spectroscopic Investigation of Metal Combustion, Aero. Engr. Lab. Rept. 586, Princeton Univ., Oct. 1961.

6. Markstein, G. H., Combustion of Metals, AIAA Journal, vol. 1, no. 3, March 1963, pp. 550-562.

7. Olson, W. T., Recombination and Condensation Processes in High Area Ratio Nozzles, ARS Journal, vol. 32, no. 5, May 1962, p. 672.

8. Hoglund, R. F., Recent Advances in Gas-Particle Nozzle Flows, ARS Journal, vol. 32, no. 5, May 1962, p. 662.

9. Povinelli, L. A., Effect of Oxidizer Particle Size on Additive Agglomeration, NASA TN D-1438, 1962.

10. Povinelli, L. A., and Ciepluch, C. C., Surface Phenomena in Solid-Propellant Combustion, Bulletin 18th Meeting JANAF-ARPA-NASA Solid Propellant Group, vol. II, 1962, pp. 387-400.

11. Watermeier, L. A., Aungst, W. P., and Pfaff, S. P., An Experimental Study of the Aluminum Additive Role in Unstable Combustion of Solid Rocket Propellants, Ninth Symposium (International) on Combustion, Academic Press, 1963, p. 316. (See also Ballistic Res. Lab. Rept. 1168, 1962, by same authors.)

12. Sehgal, R., An Experimental Investigation of a Gas-Particle System, Tech. Rept. 32-238, Jet Prop. Lab, 1962.

13. Brown, B. and McCarty, K. P., Particle Size of Condensed Oxides from Combustion of Metalized Solid Propellants, Eighth Symposium (International) on Combustion, Williams & Wilkens Co., 1962, p. 814.

TABLE I. - PROPELLANT COMPOSITIONS,

WEIGHT PERCENT

| Binder | Oxidizer | | Additive |
|---|---|---|---|
| PBAA[a] | Ammonium Perchlorate | | Aluminum |
| | Fine | Coarse | |
| 19 | 16.5 | 55.5 | 9 |
| 19 | 55.5 | 16.5 | 9 |

[a]Polybutadiene acrylic acid (epoxy crosslinked copolymer of butadiene and a carboxylic monomer).

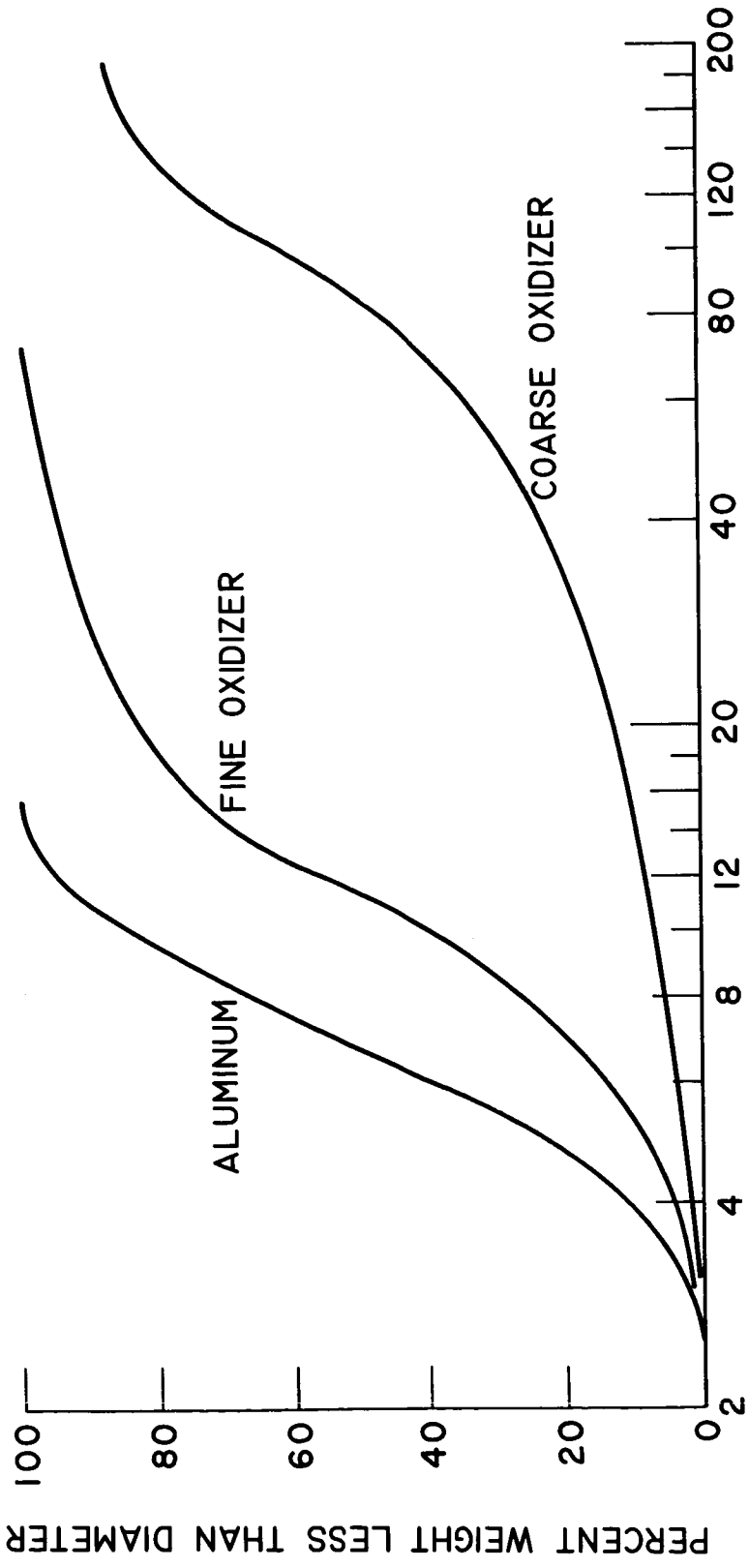


Fig. 1. - Particle size distributions of propellant ingredients.

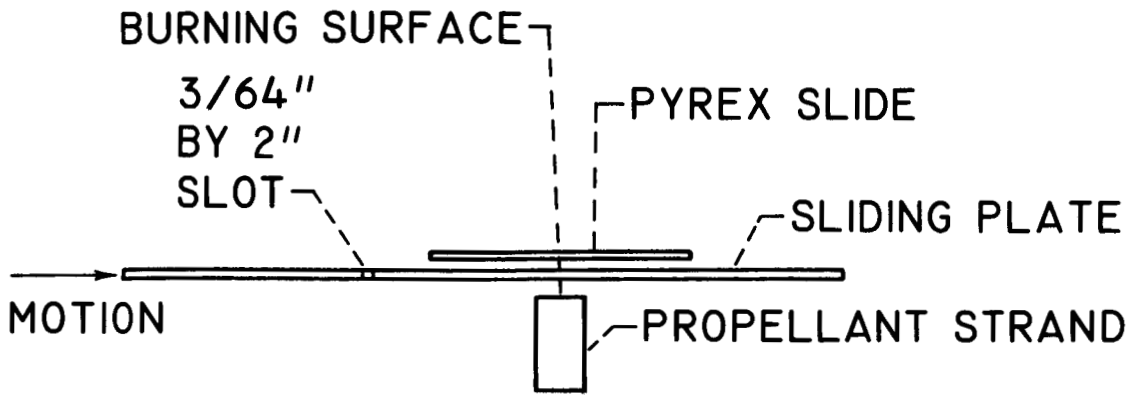


(A) END BURNING ONLY

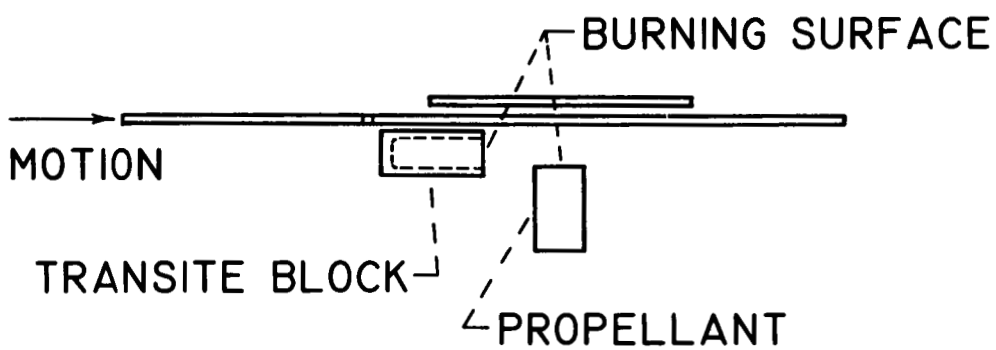


(B) END BURNING WITH CROSSFLOW

Fig. 2. - Schematic drawing of collection technique for combustion products.

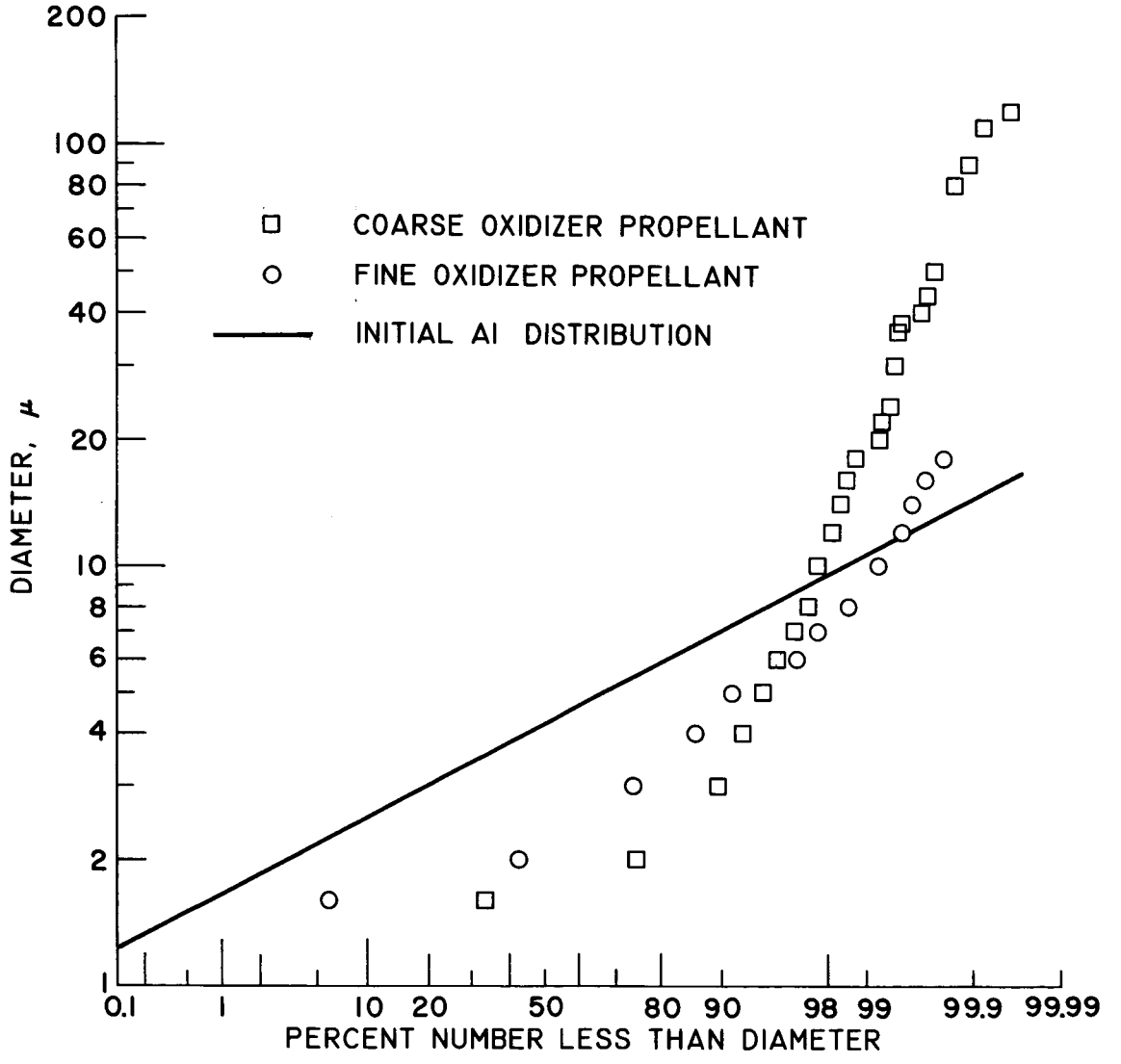


Fig. 3. - Combustion product size distribution at atmospheric pressure in a nitrogen environment.

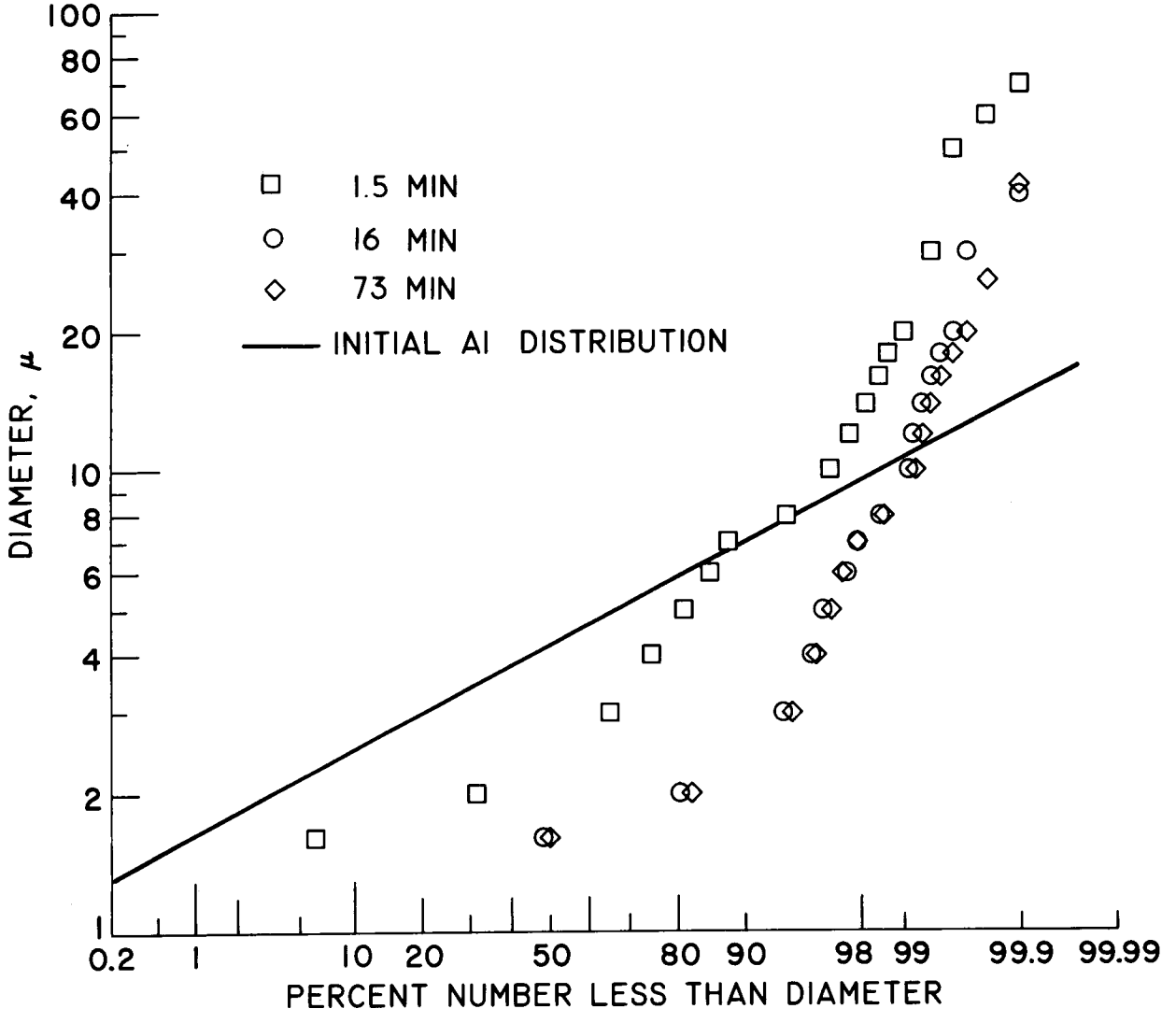


Fig. 4. - Combustion product size distribution at various vent times for coarse oxidizer propellant at 500 psi.

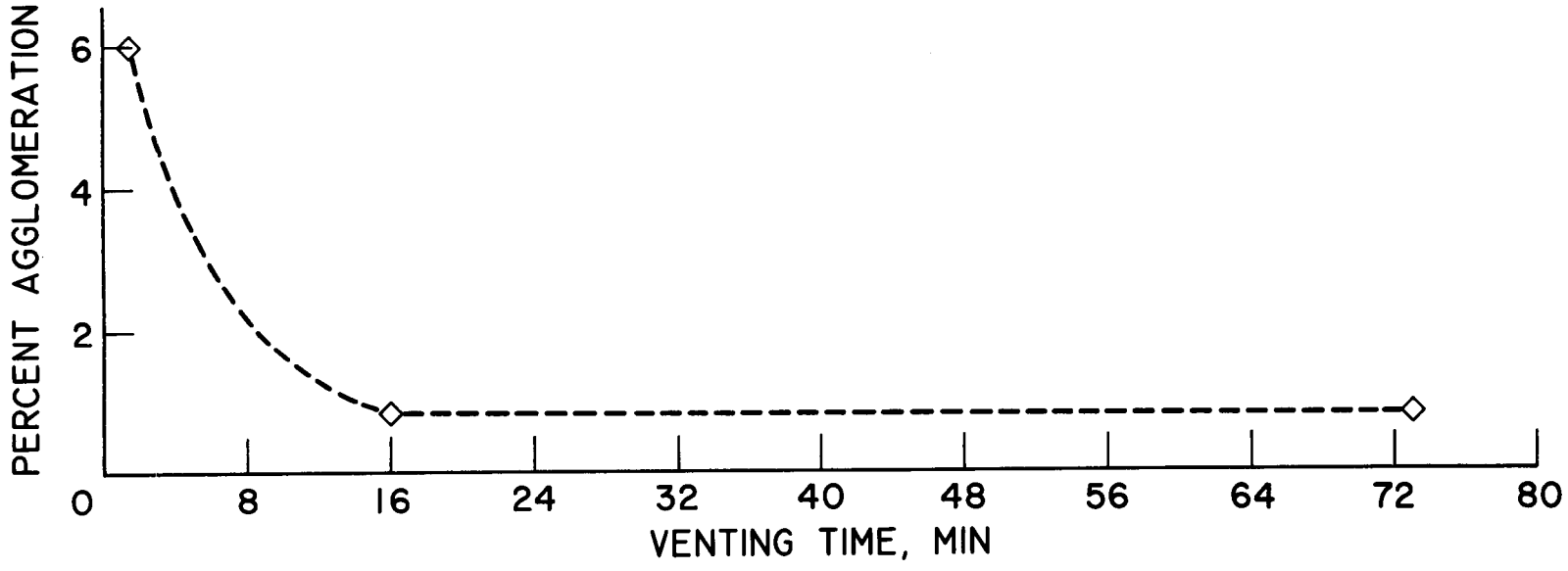


Fig. 5. - Percent agglomeration as a function of venting time for coarse oxidizer propellant at 500 psi.

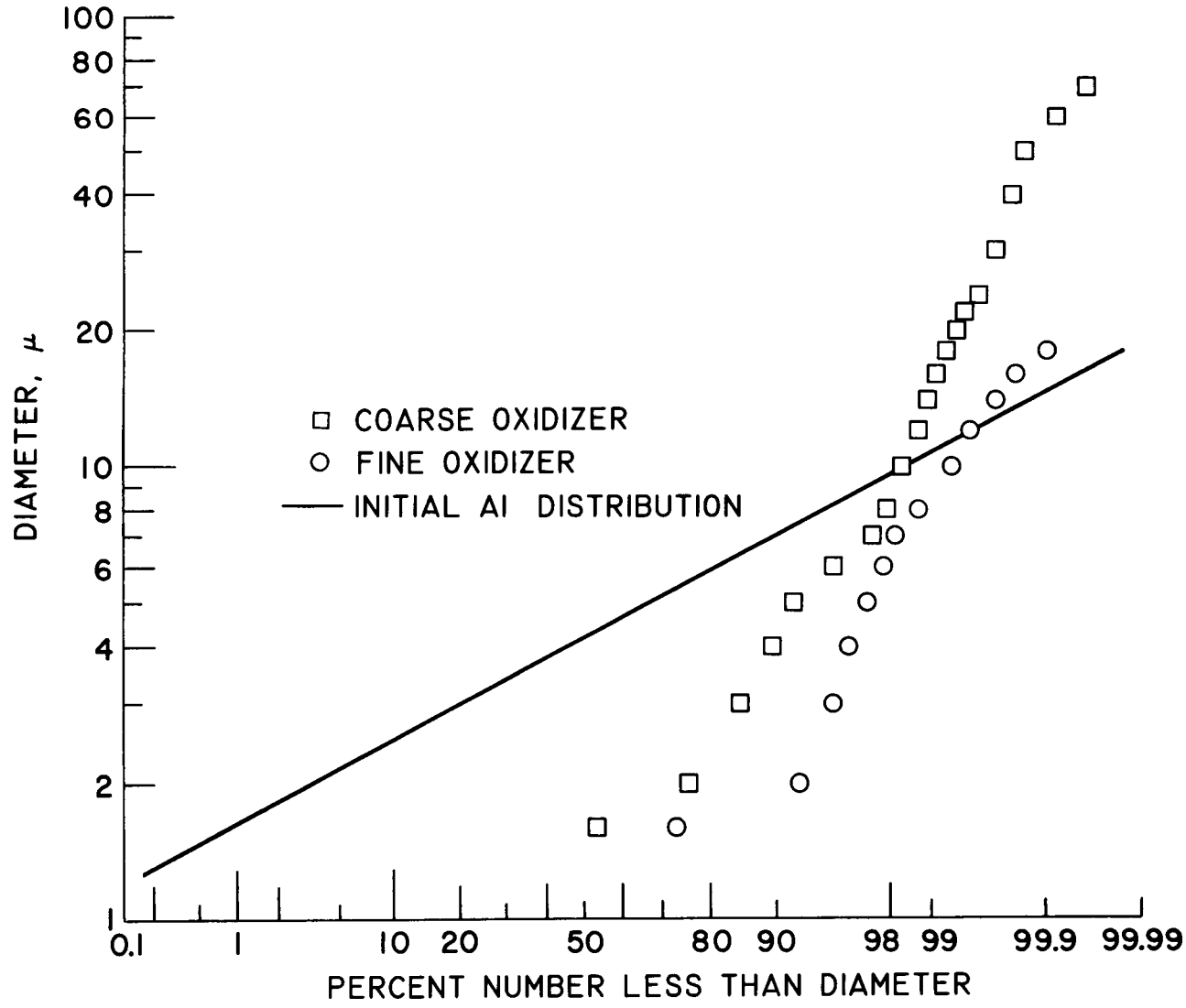


Fig. 6. - Combustion product size distribution at 50 psi.

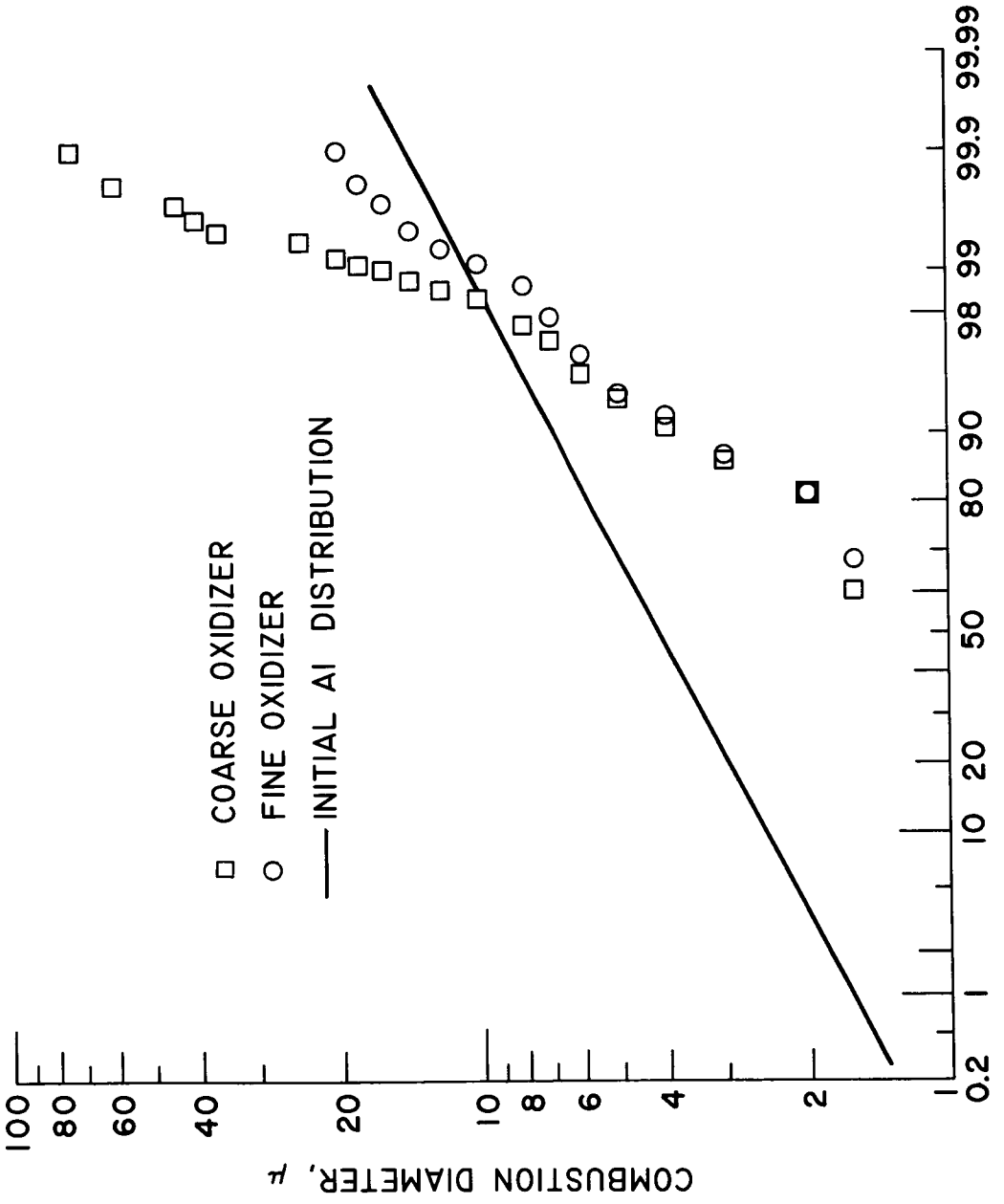


Fig. 7. - Combustion product size distribution at 100 psi.

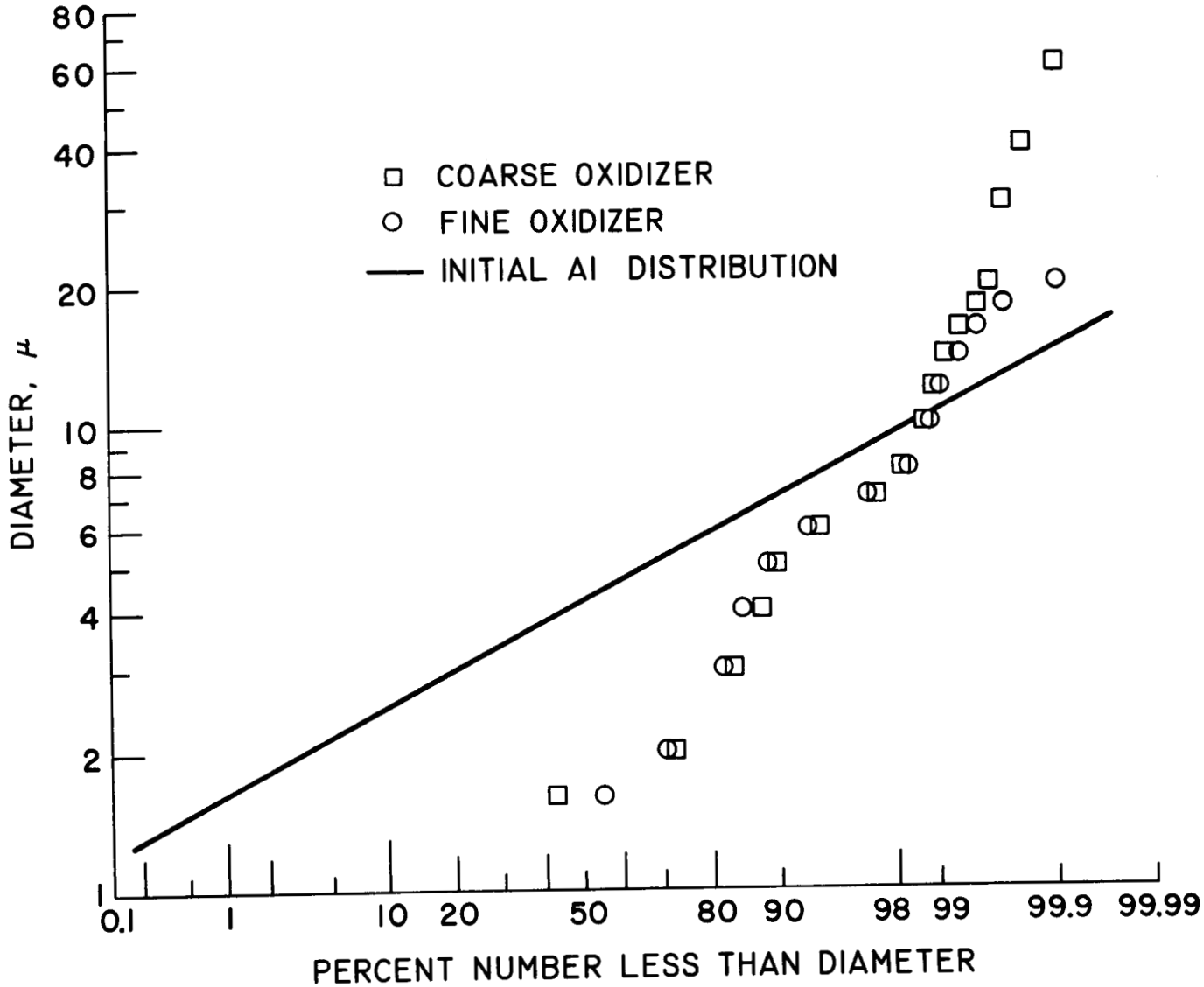


Fig. 8. - Combustion product size distribution at 250 psi.

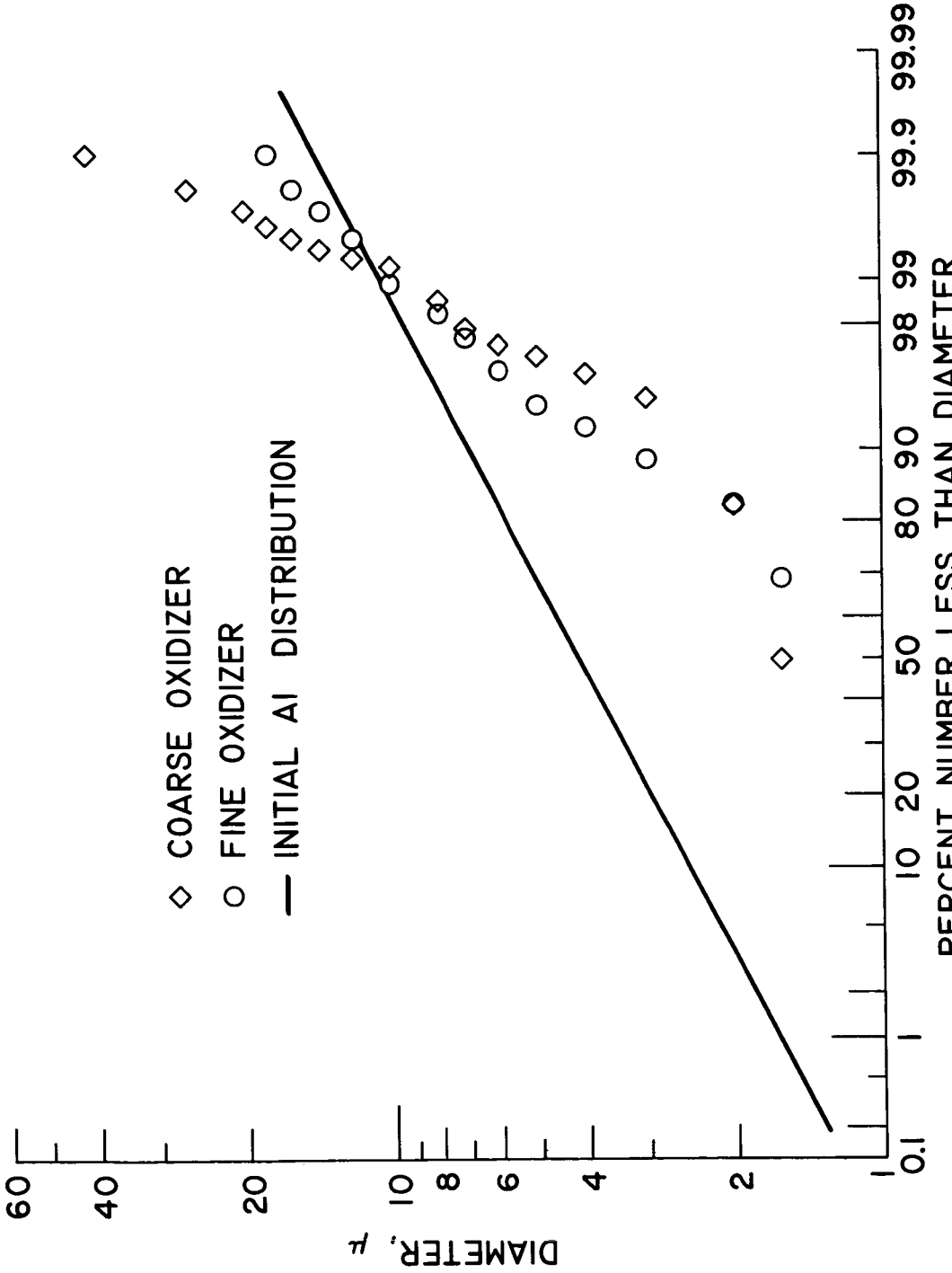


Fig. 9. - Combustion product size distribution at 500 psi.

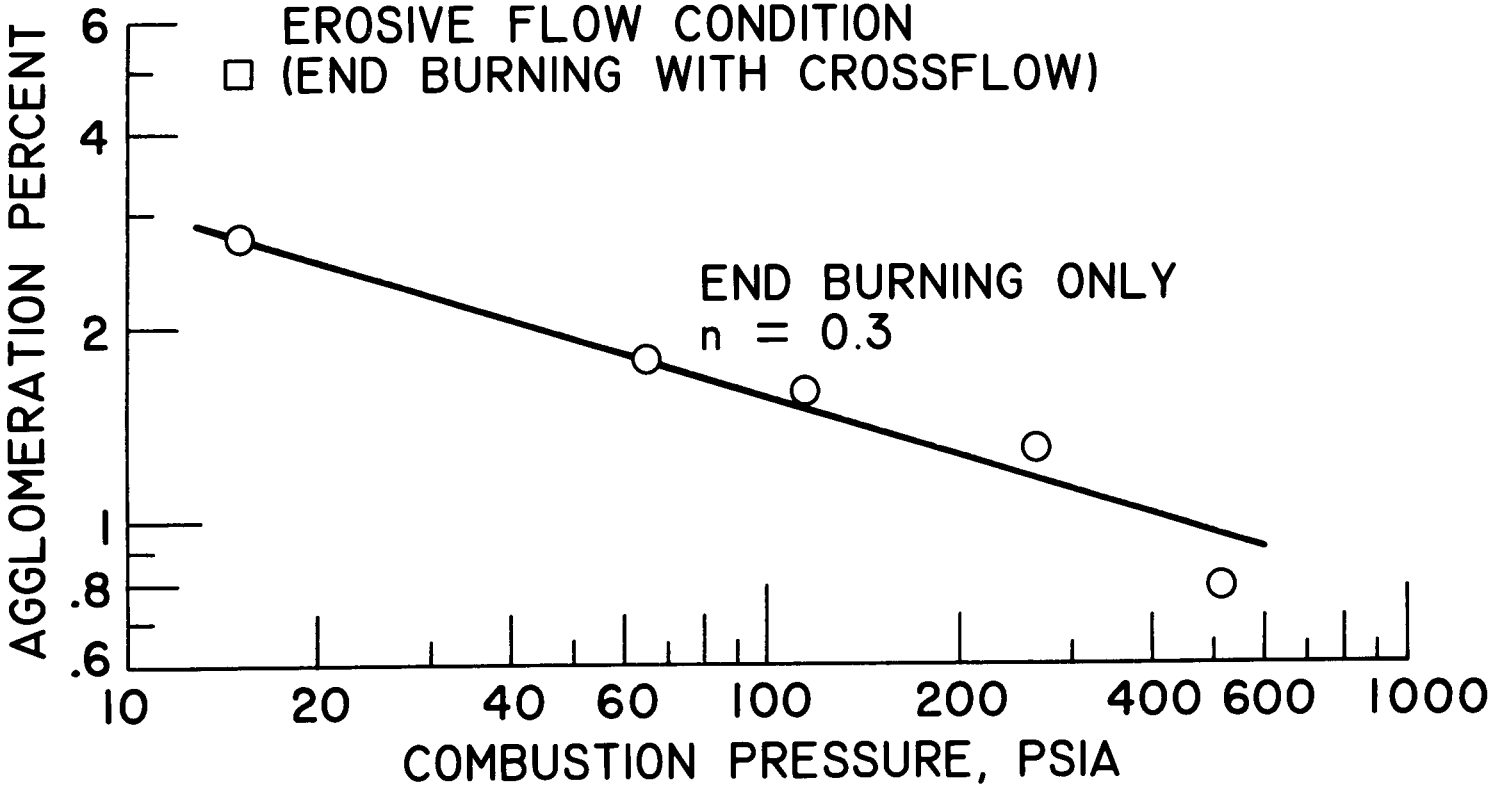


Fig. 10. - Percent agglomeration as a function of combustion pressure.

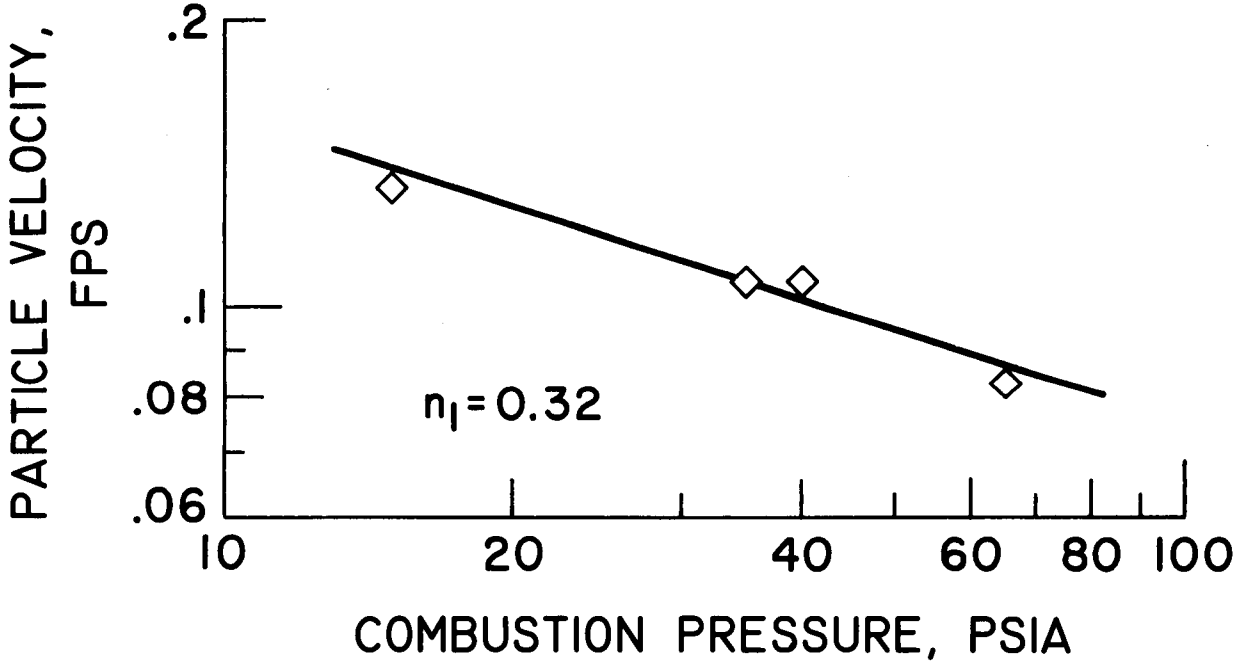


Fig. 11. - Particle velocity dependence on combustion pressure for coarse oxidzier propellant.

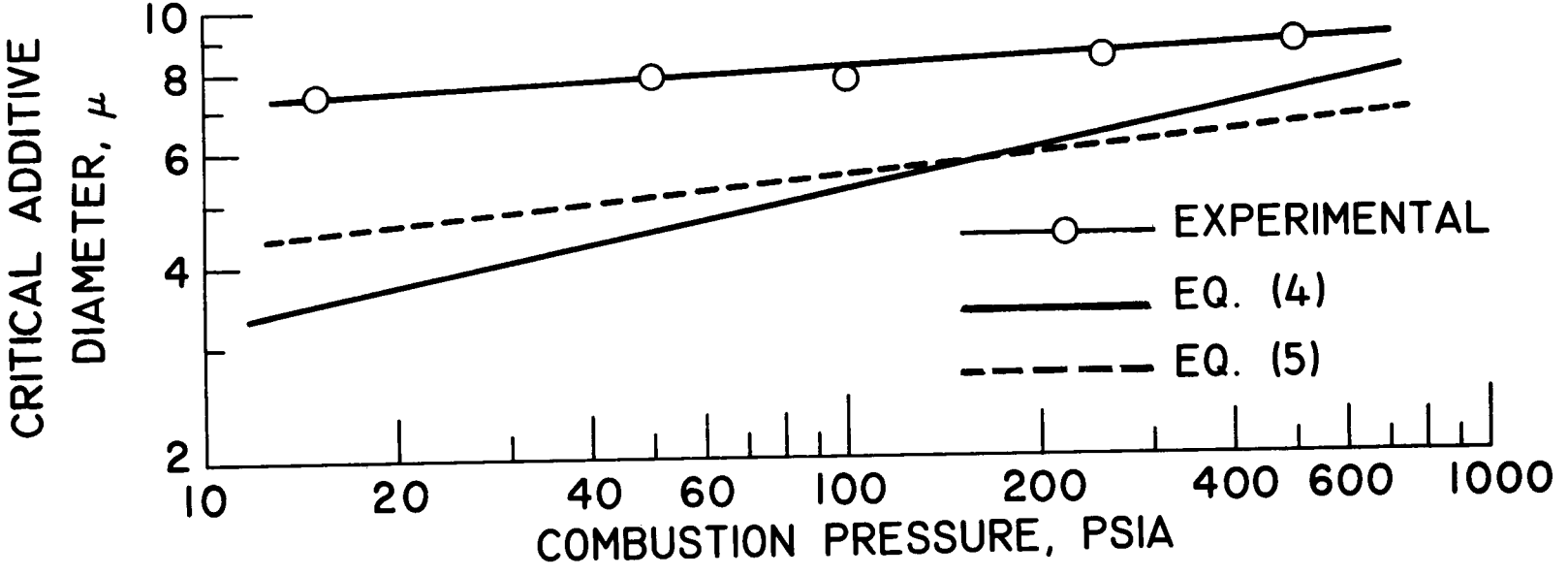


Fig. 12. - Comparison of calculated and experimental critical additive diameter for coarse oxidizer propellant.

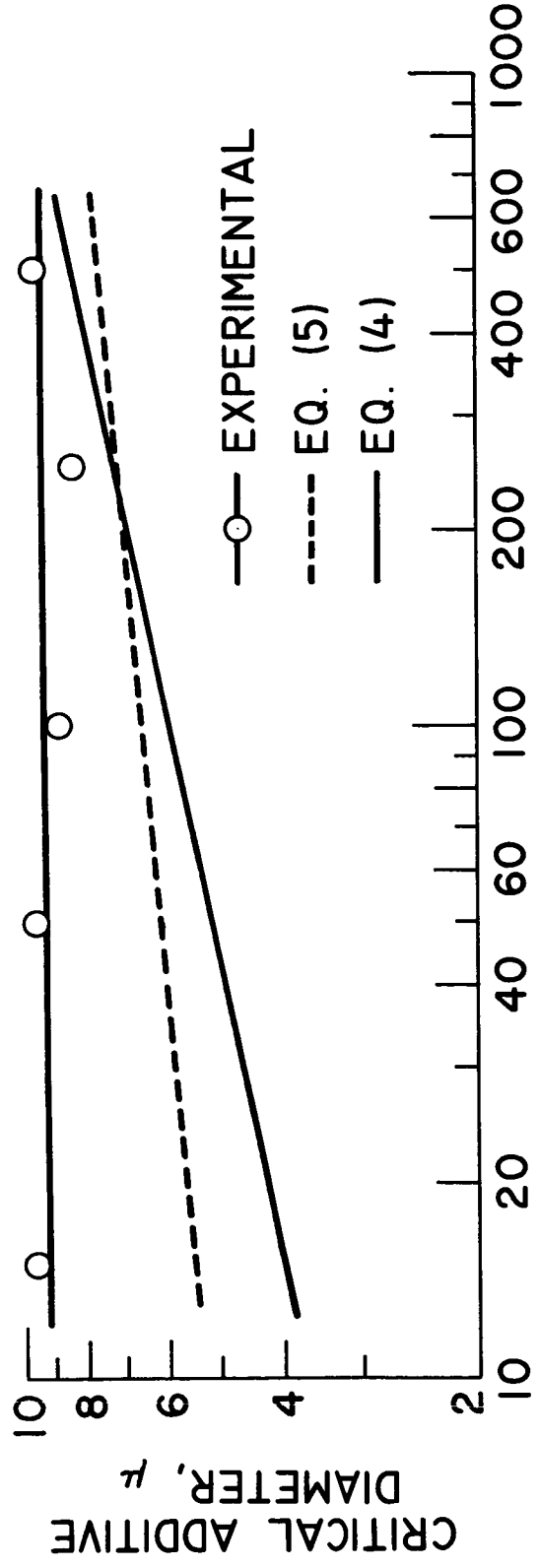


Fig. 13. - Comparison of calculated and experimental critical additive diameter for fine oxidizer propellant.

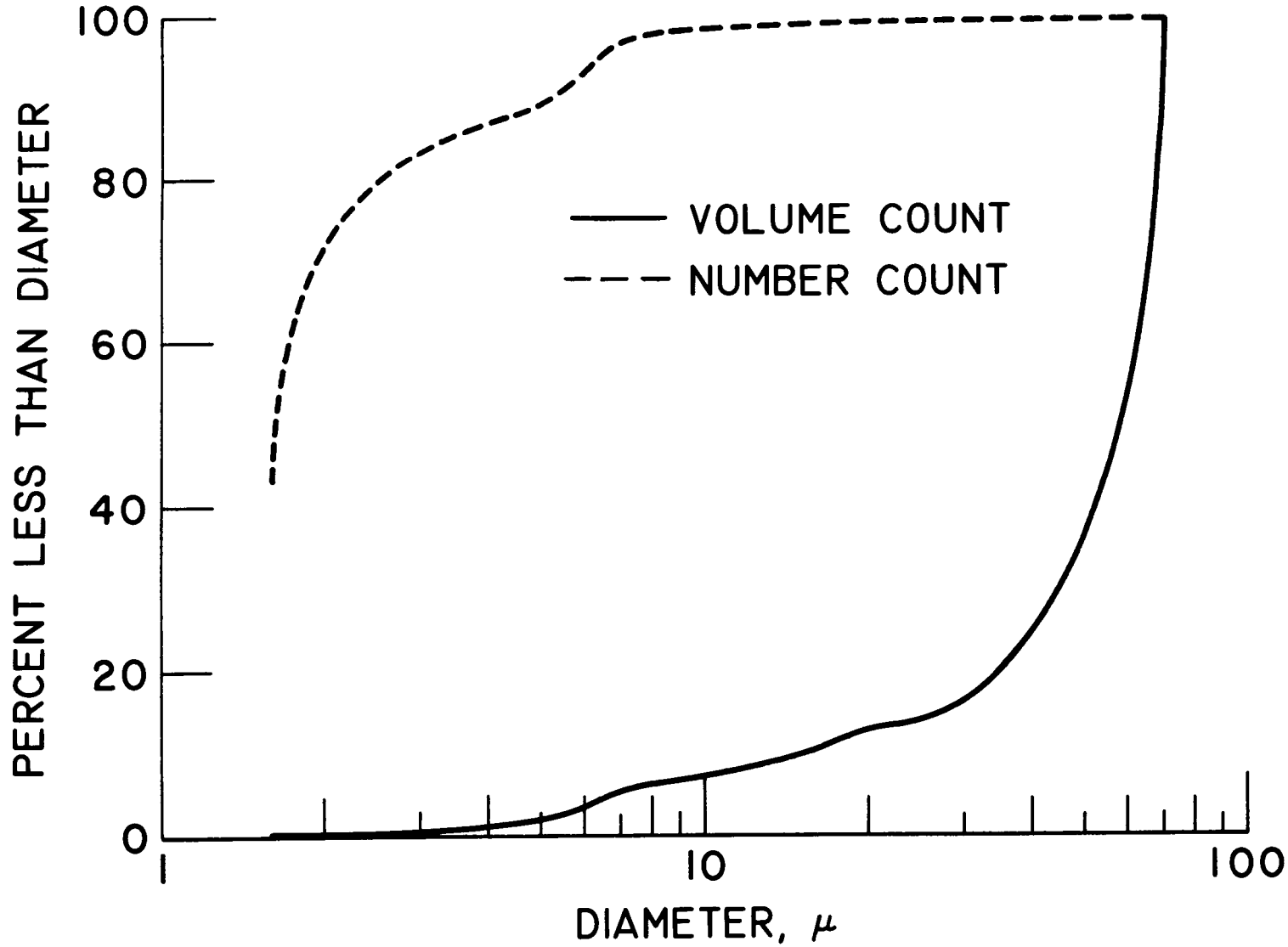


Fig. 14. - Number and volume distribution of combustion products at 250 psi.

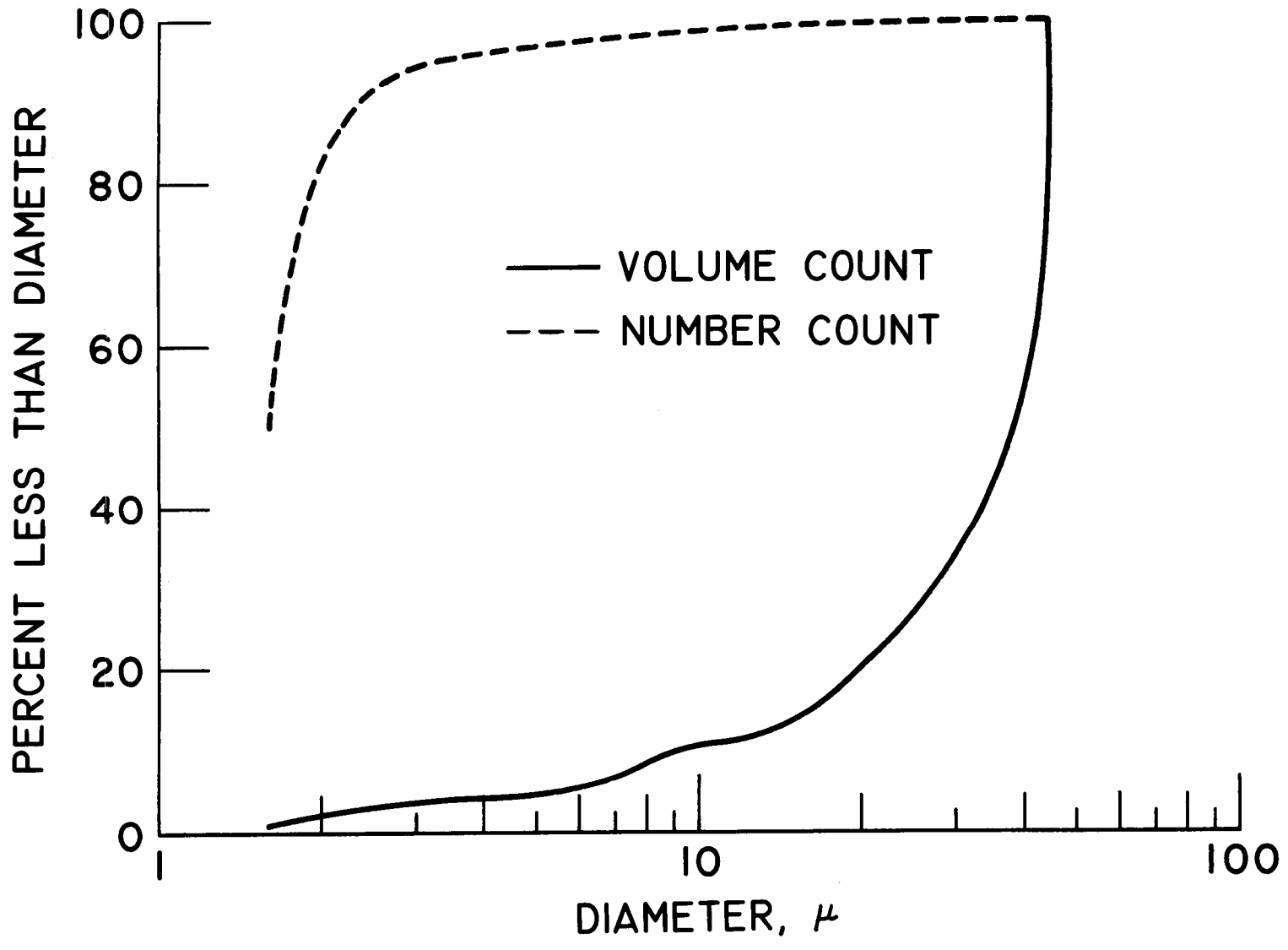


Fig. 15. - Number and volume distribution of combustion products at 500 psi.

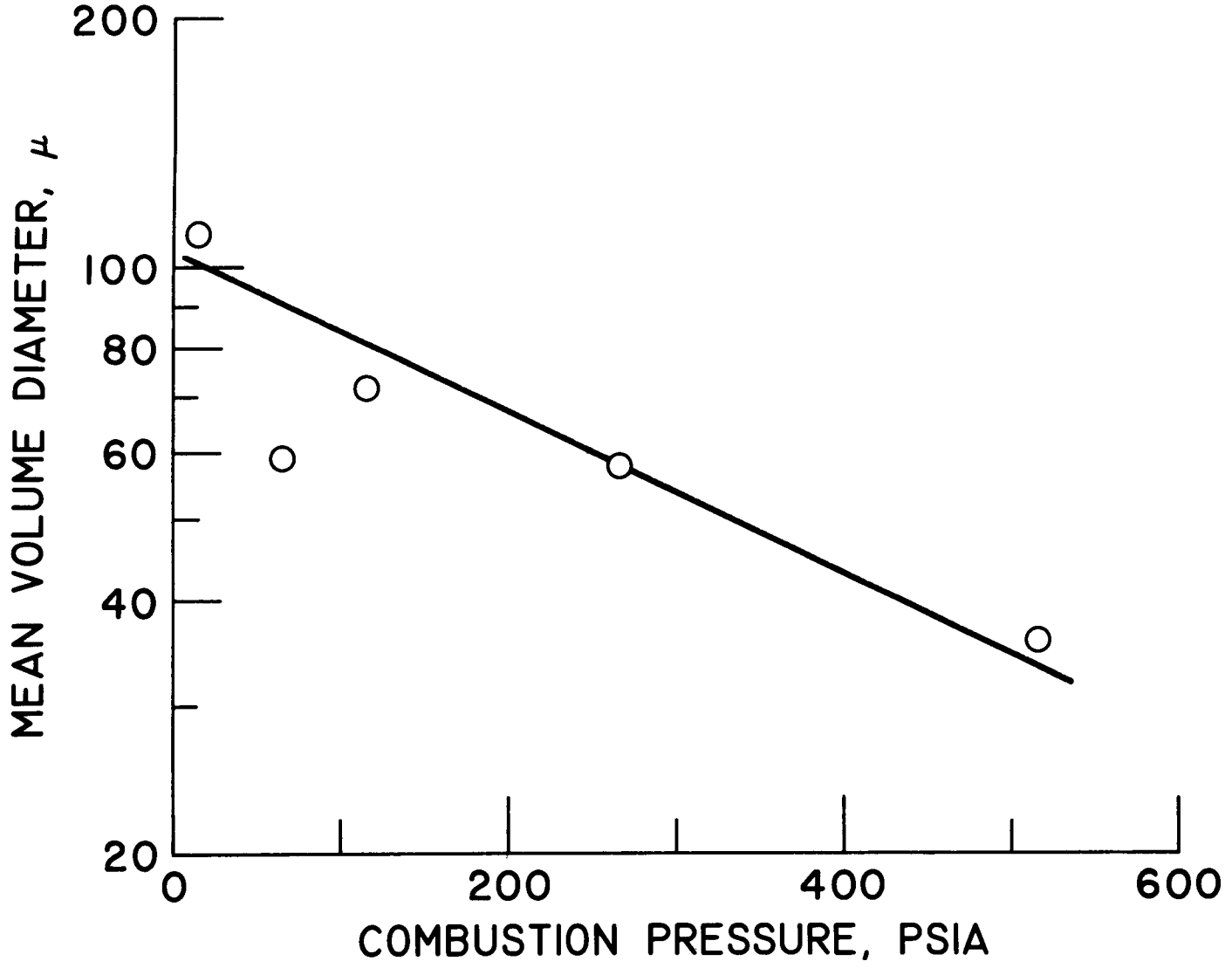


Fig. 16. - Variation of mean volume diameter with chamber pressure.

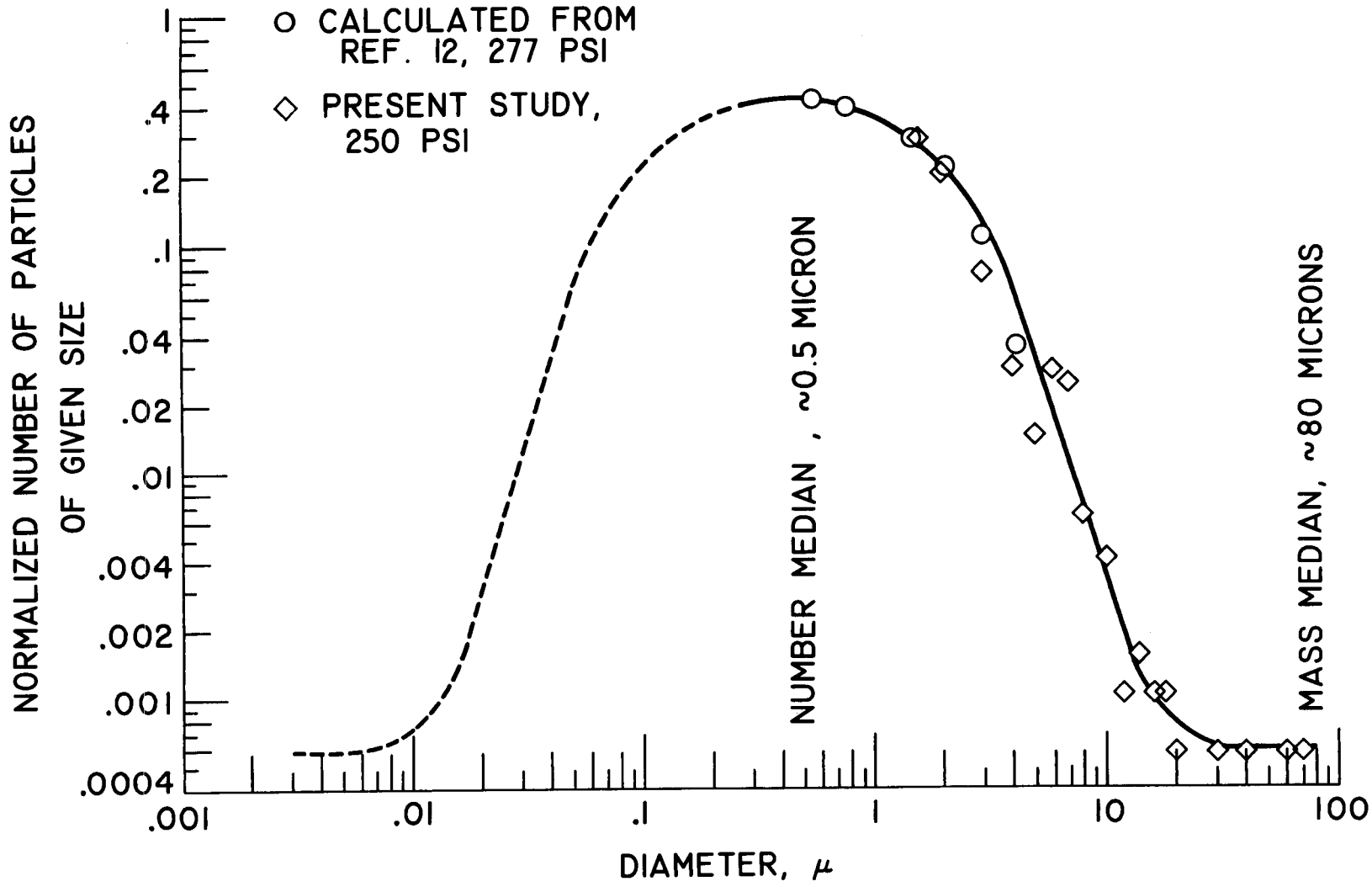


Fig. 17. - Comparison of normalized distribution from rocket samples (ref. 12) and strand burning.

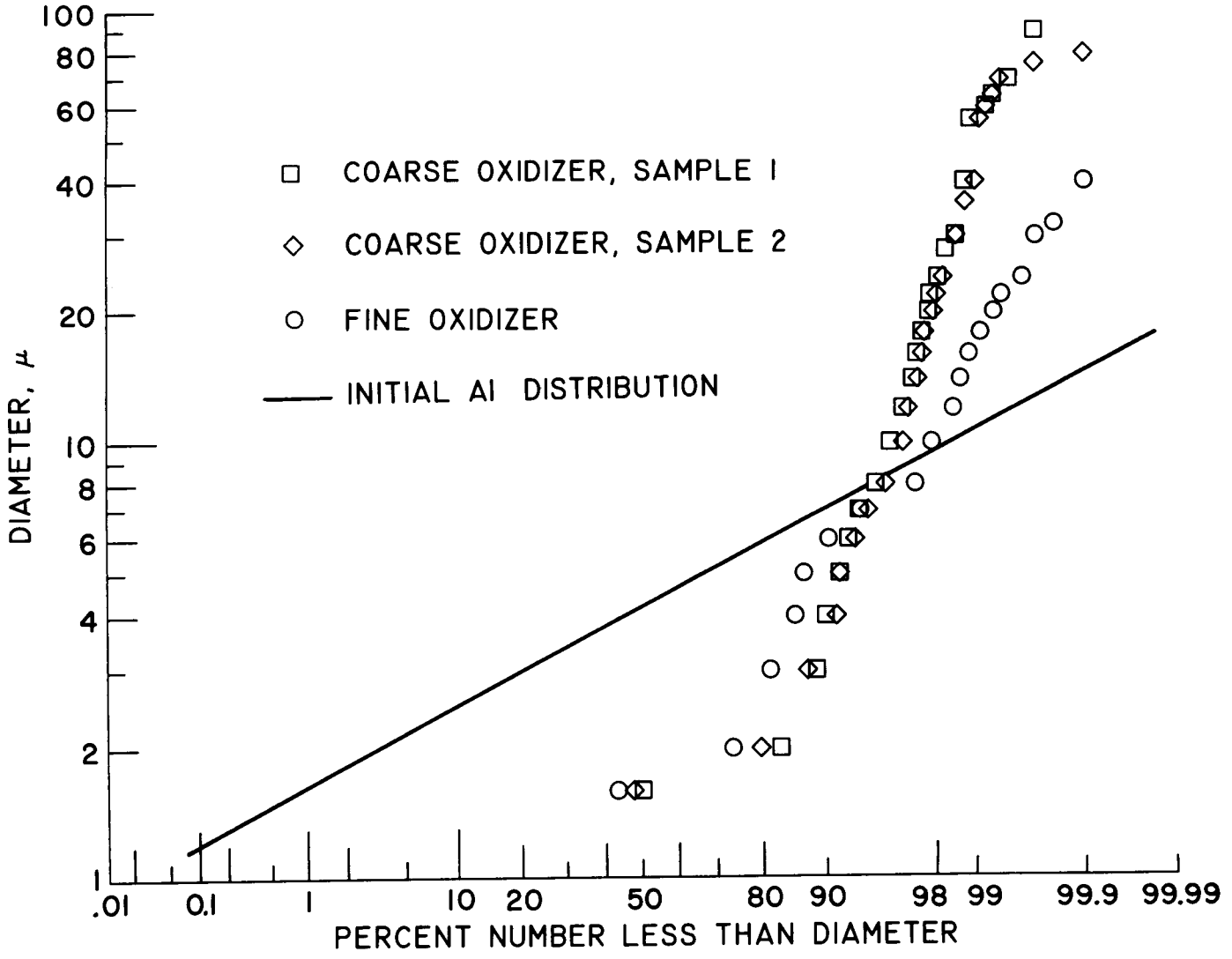


Fig. 18. - Combustion size distribution with crossflow in open air.



NASA-CLEVELAND, OHIO E-2355